

Evidence for $B^+ \rightarrow \omega l^+ \nu$

K. Abe,⁹ K. Abe,⁴⁴ N. Abe,⁴⁷ R. Abe,³⁰ T. Abe,⁹ I. Adachi,⁹ Byoung Sup Ahn,¹⁶
 H. Aihara,⁴⁶ M. Akatsu,²³ M. Asai,¹⁰ Y. Asano,⁵¹ T. Aso,⁵⁰ V. Aulchenko,² T. Aushev,¹³
 S. Bahinipati,⁵ A. M. Bakich,⁴¹ Y. Ban,³⁴ E. Banas,²⁸ S. Banerjee,⁴² A. Bay,¹⁹
 I. Bedny,² P. K. Behera,⁵² I. Bizjak,¹⁴ A. Bondar,² A. Bozek,²⁸ M. Bračko,^{21,14}
 J. Brodzicka,²⁸ T. E. Browder,⁸ M.-C. Chang,²⁷ P. Chang,²⁷ Y. Chao,²⁷ K.-F. Chen,²⁷
 B. G. Cheon,⁴⁰ R. Chistov,¹³ S.-K. Choi,⁷ Y. Choi,⁴⁰ Y. K. Choi,⁴⁰ M. Danilov,¹³
 M. Dash,⁵³ E. A. Dodson,⁸ L. Y. Dong,¹¹ R. Dowd,²² J. Dragic,²² A. Drutskoy,¹³
 S. Eidelman,² V. Eiges,¹³ Y. Enari,²³ D. Epifanov,² C. W. Everton,²² F. Fang,⁸ H. Fujii,⁹
 C. Fukunaga,⁴⁸ N. Gabyshev,⁹ A. Garmash,^{2,9} T. Gershon,⁹ G. Gokhroo,⁴² B. Golob,^{20,14}
 A. Gordon,²² M. Grosse Perdekamp,³⁶ H. Guler,⁸ R. Guo,²⁵ J. Haba,⁹ C. Hagner,⁵³
 F. Handa,⁴⁵ K. Hara,³² T. Hara,³² Y. Harada,³⁰ N. C. Hastings,⁹ K. Hasuko,³⁶
 H. Hayashii,²⁴ M. Hazumi,⁹ E. M. Heenan,²² I. Higuchi,⁴⁵ T. Higuchi,⁹ L. Hinz,¹⁹
 T. Hojo,³² T. Hokuue,²³ Y. Hoshi,⁴⁴ K. Hoshina,⁴⁹ W.-S. Hou,²⁷ Y. B. Hsiung,^{27,*}
 H.-C. Huang,²⁷ T. Igaki,²³ Y. Igarashi,⁹ T. Iijima,²³ K. Inami,²³ A. Ishikawa,²³ H. Ishino,⁴⁷
 R. Itoh,⁹ M. Iwamoto,³ H. Iwasaki,⁹ M. Iwasaki,⁴⁶ Y. Iwasaki,⁹ H. K. Jang,³⁹ R. Kagan,¹³
 H. Kakuno,⁴⁷ J. Kaneko,⁴⁷ J. H. Kang,⁵⁵ J. S. Kang,¹⁶ P. Kapusta,²⁸ M. Kataoka,²⁴
 S. U. Kataoka,²⁴ N. Katayama,⁹ H. Kawai,³ H. Kawai,⁴⁶ Y. Kawakami,²³ N. Kawamura,¹
 T. Kawasaki,³⁰ N. Kent,⁸ A. Kibayashi,⁴⁷ H. Kichimi,⁹ D. W. Kim,⁴⁰ Heejong Kim,⁵⁵
 H. J. Kim,⁵⁵ H. O. Kim,⁴⁰ Hyunwoo Kim,¹⁶ J. H. Kim,⁴⁰ S. K. Kim,³⁹ T. H. Kim,⁵⁵
 K. Kinoshita,⁵ S. Kobayashi,³⁷ P. Koppenburg,⁹ K. Korotushenko,³⁵ S. Korpar,^{21,14}
 P. Križan,^{20,14} P. Krokovny,² R. Kulasiri,⁵ S. Kumar,³³ E. Kurihara,³ A. Kusaka,⁴⁶
 A. Kuzmin,² Y.-J. Kwon,⁵⁵ J. S. Lange,^{6,36} G. Leder,¹² S. H. Lee,³⁹ T. Lesiak,²⁸
 J. Li,³⁸ A. Limosani,²² S.-W. Lin,²⁷ D. Liventsev,¹³ R.-S. Lu,²⁷ J. MacNaughton,¹²
 G. Majumder,⁴² F. Mandl,¹² D. Marlow,³⁵ T. Matsubara,⁴⁶ T. Matsuishi,²³
 H. Matsumoto,³⁰ S. Matsumoto,⁴ T. Matsumoto,⁴⁸ A. Matyja,²⁸ Y. Mikami,⁴⁵
 W. Mitaroff,¹² K. Miyabayashi,²⁴ Y. Miyabayashi,²³ H. Miyake,³² H. Miyata,³⁰
 L. C. Moffitt,²² D. Mohapatra,⁵³ G. R. Moloney,²² G. F. Moorhead,²² S. Mori,⁵¹ T. Mori,⁴⁷
 J. Mueller,^{9,†} A. Murakami,³⁷ T. Nagamine,⁴⁵ Y. Nagasaka,¹⁰ T. Nakadaira,⁴⁶ E. Nakano,³¹
 M. Nakao,⁹ H. Nakazawa,⁹ J. W. Nam,⁴⁰ S. Narita,⁴⁵ Z. Natkaniec,²⁸ K. Neichi,⁴⁴
 S. Nishida,⁹ O. Nitoh,⁴⁹ S. Noguchi,²⁴ T. Nozaki,⁹ A. Ogawa,³⁶ S. Ogawa,⁴³ F. Ohno,⁴⁷
 T. Ohshima,²³ T. Okabe,²³ S. Okuno,¹⁵ S. L. Olsen,⁸ Y. Onuki,³⁰ W. Ostrowicz,²⁸
 H. Ozaki,⁹ P. Pakhlov,¹³ H. Palka,²⁸ C. W. Park,¹⁶ H. Park,¹⁸ K. S. Park,⁴⁰ N. Parslow,⁴¹
 L. S. Peak,⁴¹ M. Pernicka,¹² J.-P. Perroud,¹⁹ M. Peters,⁸ L. E. Piilonen,⁵³ F. J. Ronga,¹⁹
 N. Root,² M. Rozanska,²⁸ H. Sagawa,⁹ S. Saitoh,⁹ Y. Sakai,⁹ H. Sakamoto,¹⁷ H. Sakaue,³¹
 T. R. Sarangi,⁵² M. Satapathy,⁵² A. Satpathy,^{9,5} O. Schneider,¹⁹ S. Schrenk,⁵
 J. Schümann,²⁷ C. Schwanda,^{9,12} A. J. Schwartz,⁵ T. Seki,⁴⁸ S. Semenov,¹³ K. Senyo,²³
 Y. Settai,⁴ R. Seuster,⁸ M. E. Sevier,²² T. Shibata,³⁰ H. Shibuya,⁴³ M. Shimoyama,²⁴
 B. Shwartz,² V. Sidorov,² V. Siegle,³⁶ J. B. Singh,³³ N. Soni,³³ S. Stanić,^{51,‡} M. Starić,¹⁴
 A. Sugi,²³ A. Sugiyama,³⁷ K. Sumisawa,⁹ T. Sumiyoshi,⁴⁸ K. Suzuki,⁹ S. Suzuki,⁵⁴
 S. Y. Suzuki,⁹ S. K. Swain,⁸ K. Takahashi,⁴⁷ F. Takasaki,⁹ B. Takeshita,³² K. Tamai,⁹
 Y. Tamai,³² N. Tamura,³⁰ K. Tanabe,⁴⁶ J. Tanaka,⁴⁶ M. Tanaka,⁹ G. N. Taylor,²²
 A. Tchouvikov,³⁵ Y. Teramoto,³¹ S. Tokuda,²³ M. Tomoto,⁹ T. Tomura,⁴⁶ S. N. Tovey,²²

K. Trabelsi,⁸ T. Tsuboyama,⁹ T. Tsukamoto,⁹ K. Uchida,⁸ S. Uehara,⁹ K. Ueno,²⁷
T. Uglov,¹³ Y. Unno,³ S. Uno,⁹ N. Uozaki,⁴⁶ Y. Ushiroda,⁹ S. E. Vahsen,³⁵ G. Varner,⁸
K. E. Varvell,⁴¹ C. C. Wang,²⁷ C. H. Wang,²⁶ J. G. Wang,⁵³ M.-Z. Wang,²⁷
M. Watanabe,³⁰ Y. Watanabe,⁴⁷ L. Widhalm,¹² E. Won,¹⁶ B. D. Yabsley,⁵³ Y. Yamada,⁹
A. Yamaguchi,⁴⁵ H. Yamamoto,⁴⁵ T. Yamanaka,³² Y. Yamashita,²⁹ Y. Yamashita,⁴⁶
M. Yamauchi,⁹ H. Yanai,³⁰ Heyoung Yang,³⁹ J. Yashima,⁹ P. Yeh,²⁷ M. Yokoyama,⁴⁶
K. Yoshida,²³ Y. Yuan,¹¹ Y. Yusa,⁴⁵ H. Yuta,¹ C. C. Zhang,¹¹ J. Zhang,⁵¹ Z. P. Zhang,³⁸
Y. Zheng,⁸ V. Zhilich,² Z. M. Zhu,³⁴ T. Ziegler,³⁵ D. Žontar,^{20, 14} and D. Zürcher¹⁹

(The Belle Collaboration)

¹*Aomori University, Aomori*

²*Budker Institute of Nuclear Physics, Novosibirsk*

³*Chiba University, Chiba*

⁴*Chuo University, Tokyo*

⁵*University of Cincinnati, Cincinnati, Ohio 45221*

⁶*University of Frankfurt, Frankfurt*

⁷*Gyeongsang National University, Chinju*

⁸*University of Hawaii, Honolulu, Hawaii 96822*

⁹*High Energy Accelerator Research Organization (KEK), Tsukuba*

¹⁰*Hiroshima Institute of Technology, Hiroshima*

¹¹*Institute of High Energy Physics,*

Chinese Academy of Sciences, Beijing

¹²*Institute of High Energy Physics, Vienna*

¹³*Institute for Theoretical and Experimental Physics, Moscow*

¹⁴*J. Stefan Institute, Ljubljana*

¹⁵*Kanagawa University, Yokohama*

¹⁶*Korea University, Seoul*

¹⁷*Kyoto University, Kyoto*

¹⁸*Kyungpook National University, Taegu*

¹⁹*Institut de Physique des Hautes Énergies, Université de Lausanne, Lausanne*

²⁰*University of Ljubljana, Ljubljana*

²¹*University of Maribor, Maribor*

²²*University of Melbourne, Victoria*

²³*Nagoya University, Nagoya*

²⁴*Nara Women's University, Nara*

²⁵*National Kaohsiung Normal University, Kaohsiung*

²⁶*National Lien-Ho Institute of Technology, Miao Li*

²⁷*Department of Physics, National Taiwan University, Taipei*

²⁸*H. Niewodniczanski Institute of Nuclear Physics, Krakow*

²⁹*Nihon Dental College, Niigata*

³⁰*Niigata University, Niigata*

³¹*Osaka City University, Osaka*

³²*Osaka University, Osaka*

³³*Panjab University, Chandigarh*

³⁴*Peking University, Beijing*

³⁵*Princeton University, Princeton, New Jersey 08545*

³⁶*RIKEN BNL Research Center, Upton, New York 11973*

- ³⁷*Saga University, Saga*
³⁸*University of Science and Technology of China, Hefei*
³⁹*Seoul National University, Seoul*
⁴⁰*Sungkyunkwan University, Suwon*
⁴¹*University of Sydney, Sydney NSW*
⁴²*Tata Institute of Fundamental Research, Bombay*
⁴³*Toho University, Funabashi*
⁴⁴*Tohoku Gakuin University, Tagajo*
⁴⁵*Tohoku University, Sendai*
⁴⁶*Department of Physics, University of Tokyo, Tokyo*
⁴⁷*Tokyo Institute of Technology, Tokyo*
⁴⁸*Tokyo Metropolitan University, Tokyo*
⁴⁹*Tokyo University of Agriculture and Technology, Tokyo*
⁵⁰*Toyama National College of Maritime Technology, Toyama*
⁵¹*University of Tsukuba, Tsukuba*
⁵²*Utkal University, Bhubaneswer*
⁵³*Virginia Polytechnic Institute and State University, Blacksburg, Virginia 24061*
⁵⁴*Yokkaichi University, Yokkaichi*
⁵⁵*Yonsei University, Seoul*

Abstract

We have searched for the decay $B^+ \rightarrow \omega l^+ \nu$ in 78 fb⁻¹ of $\Upsilon(4S)$ data (85.0 million $B\bar{B}$ events) accumulated with the Belle detector. The final state is fully reconstructed using the ω decay into $\pi^+ \pi^- \pi^0$ and detector hermeticity to estimate the neutrino momentum. 155 ± 47 signal events are found in the data, corresponding to a branching fraction of $(1.3 \pm 0.4 \pm 0.2 \pm 0.3) \cdot 10^{-4}$, where the first two errors are statistical and systematic. The third error is due to the estimated form-factor uncertainty. (This result is preliminary.)

PACS numbers: 13.25.Hw

INTRODUCTION

The magnitude of V_{ub} plays an important role in probing the unitarity of the Cabbibo-Kobayashi-Maskawa (CKM) matrix [1]. At present, experimental constraints on $|V_{ub}|$ come mainly from the analysis of the decay $B \rightarrow X_u l \nu$. Both inclusive approaches (sensitive to all $X_u l \nu$ final states within a given region of phase space) and the exclusive reconstruction of specific final states have been attempted. For the latter, Belle has previously obtained preliminary results for the decays $B \rightarrow \pi l \nu$ and $B \rightarrow \rho l \nu$ [2]. This article presents a study of the decay $B^+ \rightarrow \omega l^+ \nu$, which has not been observed so far [3].

Using a 78 fb^{-1} dataset recorded on the $\Upsilon(4S)$ resonance (85.0 million $B\bar{B}$ events), events with a single (undetected) neutrino are selected and the neutrino momentum is inferred from detector hermeticity. The neutrino candidate is combined with an identified lepton (electron or muon) and an ω (reconstructed through $\omega \rightarrow \pi^+ \pi^- \pi^0$) and the final state is reconstructed. The $B \rightarrow \omega l \nu$ yield and the remaining background are determined by a binned maximum likelihood fit.

EXPERIMENTAL PROCEDURE

KEKB and the Belle detector

Belle is located at KEKB, an asymmetric e^+e^- collider operating at the center-of-mass energy of the $\Upsilon(4S)$ resonance. The detector is described in detail elsewhere [4]. It is a large-solid-angle magnetic spectrometer that consists of a three-layer silicon vertex detector (SVD), a 50-layer central drift chamber (CDC), an array of aerogel threshold Čerenkov counters (ACC), a barrel-like arrangement of time-of-flight scintillation counters (TOF), and an electromagnetic calorimeter comprised of CsI(Tl) crystals (ECL) located inside a super-conducting solenoid coil that provides a 1.5 T magnetic field.

The responses of the ECL, CDC (dE/dx) and ACC detectors are combined to provide clean electron identification. Muons are identified in the instrumented iron flux-return (KLM) located outside of the coil. Charged hadron identification relies on the information from the CDC, ACC and TOF sub-detectors.

Dataset

The $\Upsilon(4S)$ dataset used for this study corresponds to an integrated luminosity of 78.13 fb^{-1} and contains $(85.0 \pm 0.5) \cdot 10^6$ $B\bar{B}$ events. Continuum background is subtracted using 8.83 fb^{-1} of data taken below the resonance.

A full detector simulation based on GEANT is applied to Monte Carlo events. This analysis uses background Monte Carlo samples, equivalent to about three times the integrated luminosity. Monte Carlo data for the signal decay, $B^+ \rightarrow \omega l^+ \nu$, are generated with three different form-factor models: ISGW2 (quark model [5]), UKQCD (quenched lattice QCD calculation [6]) and LCSR (light cone sum rules [7]). To model the cross-feed from other $B \rightarrow X_u l \nu$ decays, Monte Carlo samples generated with the ISGW2 and the De Fazio-Neubert model [8] are used.

Neutrino reconstruction

Events passing the hadronic selection are required to contain a single lepton (electron or muon) with a c.m. momentum p_l^* greater than 1.3 GeV/ c . In this momentum range, electrons (muons) are selected with an efficiency of 92% (89%) and a pion fake rate of 0.25% (1.4%).

The missing four-momentum is computed for selected events,

$$\begin{aligned}\vec{p}_{miss} &= \vec{p}_{HER} + \vec{p}_{LER} - \sum_i \vec{p}_i, \\ E_{miss} &= E_{HER} + E_{LER} - \sum_i E_i,\end{aligned}\tag{1}$$

where the sum runs over all reconstructed charged tracks and photons. The indices HER and LER refer to the high energy and the low energy rings, respectively. To reject events in which the missing momentum misrepresents the neutrino momentum, the following selections are applied. Events with a large charge imbalance are eliminated, $|Q_{tot}| < 3e$, and the direction of the missing momentum is required to lie within the ECL acceptance, $17^\circ < \theta_{miss} < 150^\circ$. The missing mass squared, $m_{miss}^2 = E_{miss}^2 - \vec{p}_{miss}^2$, is required to be consistent with the neutrino hypothesis, $|m_{miss}^2| < 3 \text{ GeV}^2/c^4$.

After applying these cuts, the resolution in p_{miss} is around 140 MeV/ c for generic $B \rightarrow X_u l \nu$ events. As the energy resolution is worse than the momentum resolution, the neutrino four-momentum is taken to be $(p_{miss}, \vec{p}_{miss})$. The efficiency of the combined event selection and neutrino reconstruction cuts is about 17% for $B \rightarrow X_u l \nu$ events.

Final state reconstruction

Pairs of γ 's are combined to form π^0 candidates ($E_\gamma > 30 \text{ MeV}$, $120 < m(\gamma\gamma) < 150 \text{ MeV}/c^2$). The decay $\omega \rightarrow \pi^+\pi^-\pi^0$ (branching ratio: $(89.1 \pm 0.7)\%$ [9]) is reconstructed from all possible combinations of one π^0 with two oppositely charged tracks. Combinations with a charged track identified as a kaon are rejected and the following selections are imposed: $p_\omega^* > 300 \text{ MeV}/c$, $703 < m(\pi^+\pi^-\pi^0) < 863 \text{ MeV}/c^2$. Combinations located far from the center of the Dalitz plot are removed by requiring the Dalitz amplitude, $A \propto |\vec{p}_{\pi^+} \times \vec{p}_{\pi^-}|$, to be larger than half of its maximum value.

The lepton in the event is combined with the ω candidate and the neutrino, and the lepton momentum requirement is tightened, $1.8 < p_l^* < 2.7 \text{ GeV}/c$. To reject combinations inconsistent with signal decay kinematics, the cut $|\cos \theta_{BY}| < 1.1$ is imposed,

$$\cos \theta_{BY} = \frac{2E_B^* E_Y^* - m_B^2 - m_Y^2}{2p_B^* p_Y^*},\tag{2}$$

where E_B^* , p_B^* and m_B are fixed to their nominal values, $\sqrt{E_{HER} E_{LER}}$, $\sqrt{E_B^{*2} - m_B^2}$ and 5.279 GeV/ c^2 , respectively. The variables E_Y^* , p_Y^* and m_Y are the measured c.m. energy, momentum and mass of the $Y = \omega + l$ system, respectively. For well-reconstructed signal events, $\cos \theta_{BY}$ is the cosine of the angle between the B and the Y system and lies between -1 and $+1$ while for background, a significant fraction is outside this interval.

For each $\omega l\nu$ candidate, the beam-constrained mass m_{bc} and ΔE are calculated ($E_{beam}^* = \sqrt{E_{HER}E_{LER}}$),

$$\begin{aligned} m_{bc} &= \sqrt{(E_{beam}^*)^2 - |\vec{p}_\omega^* + \vec{p}_l^* + \vec{p}_\nu^*|^2} , \\ \Delta E &= E_{beam}^* - (E_\omega^* + E_l^* + E_\nu^*) , \end{aligned} \quad (3)$$

and candidates in the range $m_{bc} > 5.23 \text{ GeV}/c^2$ and $|\Delta E| < 1.08 \text{ GeV}$ are selected. On average, 2.5 combinations per event satisfy all cuts and we choose the one with the largest ω momentum in the c.m. frame. This choice is correct in 77% of the cases.

Continuum suppression

The background from continuum $e^+e^- \rightarrow q\bar{q}$ events, $q = u, d, s, c$, is suppressed using three variables that exploit the fact that, in the $\Upsilon(4S)$ frame, the two B mesons are produced nearly at rest and that therefore $B\bar{B}$ events are nearly spherical while continuum events have a more jet-like topology. These variables are:

- The ratio R_2 of the second to the zeroth Fox-Wolfram moment [10]. This ratio tends to be close to zero (unity) for spherical (jet-like) events. (The cut $R_2 < 0.4$ is imposed at the event selection level.)
- The cosine of θ_{thrust} , where θ_{thrust} is the angle between the thrust axis of the ωl system and the thrust axis of the rest of the event.
- A Fisher discriminant that selects events with a uniform energy distribution around the lepton direction [11]. The input variables are the charged and neutral energy in nine cones of equal solid angle around the lepton momentum axis.

A cut on the likelihood ratio combining the three variables is imposed. This selection is 56% efficient for $B^+ \rightarrow \omega l^+ \nu$ events while it eliminates 92% of the continuum background remaining after the $R_2 < 0.4$ cut.

The fit

The signal yield and the remaining background are determined by a binned maximum likelihood fit in the ΔE vs. $m(\pi^+\pi^-\pi^0)$ plane taking into account the finite Monte Carlo statistics [12]. 9 bins in ΔE (bin width: 240 MeV) and 8 bins in $m(\pi^+\pi^-\pi^0)$ (bin width: 20 MeV/ c^2) are used. This fit is performed simultaneously in three bins of lepton momentum, $1.8 < p_l^* < 2.1 \text{ GeV}/c$, $2.1 < p_l^* < 2.4 \text{ GeV}/c$ and $2.4 < p_l^* < 2.7 \text{ GeV}/c$.

Five components are fitted to the data: the $B^+ \rightarrow \omega l^+ \nu$ signal, $B \rightarrow X_u l \nu$ background, $B \rightarrow X_c l \nu$ background, fake and non- B decay lepton background and continuum. The shapes of the first four components are determined from simulation, while the shape of the continuum component is given by the off-resonance data. The normalizations of the $B^+ \rightarrow \omega l^+ \nu$, the $B \rightarrow X_u l \nu$ and the $B \rightarrow X_c l \nu$ components are floated in the fit, while the other components are fixed (Table I, Fig. 1).

BELLE

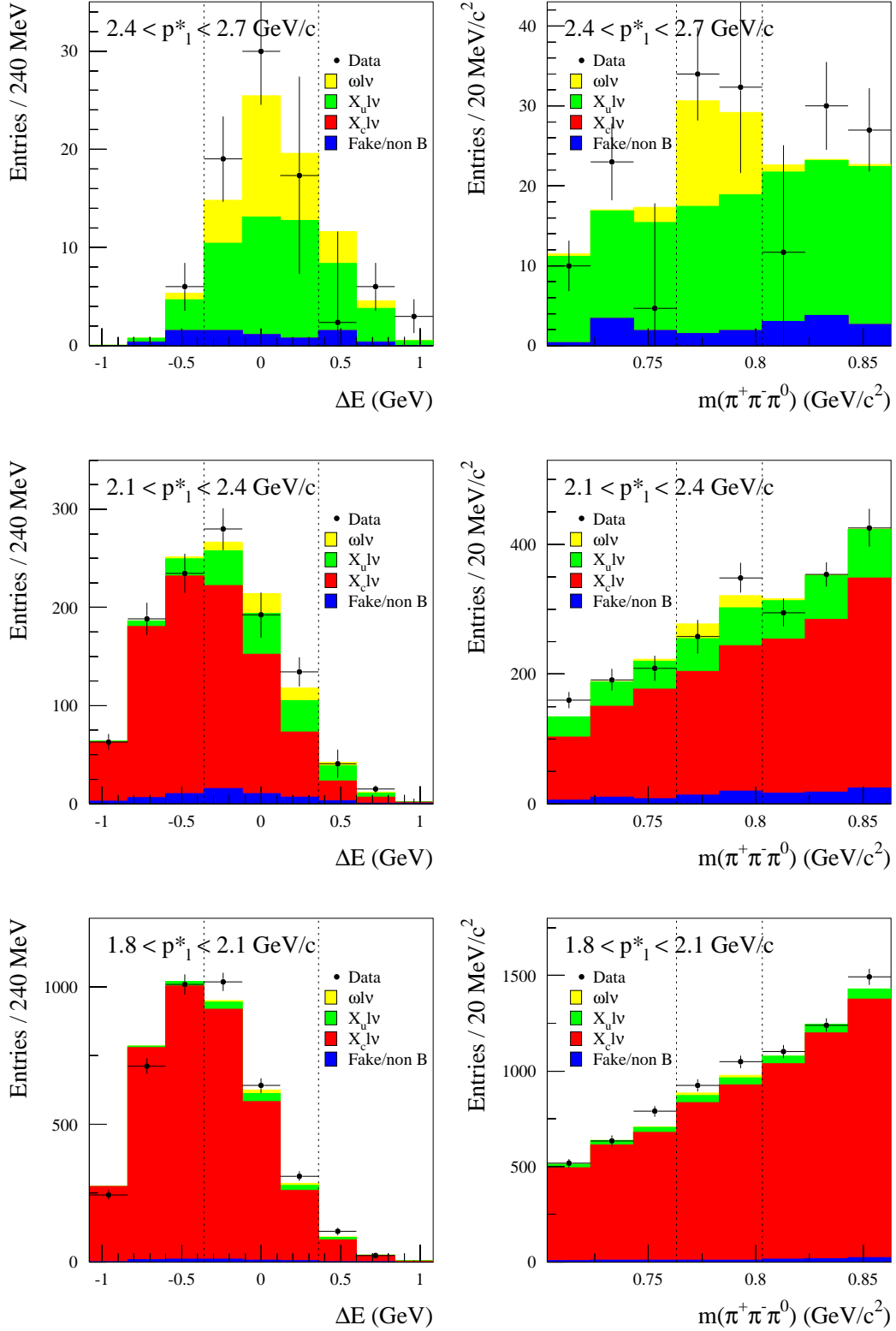


FIG. 1: The result of the fit assuming ISGW2 form-factors for $B^+ \rightarrow \omega l^+ \nu$. The ΔE and $m(\pi^+ \pi^- \pi^0)$ distributions in each p_l^* bin are shown. The data points are continuum subtracted on-resonance data, the histograms are the components of the fit, as described in the text.

	$1.8 < p_l^* < 2.1 \text{ GeV}/c$	$2.1 < p_l^* < 2.4 \text{ GeV}/c$	$2.4 < p_l^* < 2.7 \text{ GeV}/c$
data	1990	667	75
$B^+ \rightarrow \omega l^+ \nu$	41 ± 13	68 ± 21	35 ± 11
$B \rightarrow X_u l \nu$	61 ± 28	82 ± 28	21 ± 5
$B \rightarrow X_c l \nu$	1743 ± 36	415 ± 14	0
fake, non B	19 ± 3	33 ± 4	3 ± 1
continuum	17 ± 12	61 ± 23	9 ± 9
sum	1881 ± 49	659 ± 44	68 ± 15

TABLE I: The result of the fit assuming ISGW2 form-factors for $B^+ \rightarrow \omega l^+ \nu$. For each p_l^* bin, the number of events in the signal window, $763 < m(\pi^+ \pi^- \pi^0) < 803 \text{ MeV}/c^2$ and $|\Delta E| < 360 \text{ MeV}$, are shown for the data and the different components of the fit.

form-factor model	signal yield	$\mathcal{B}(B^+ \rightarrow \omega l^+ \nu)$	χ^2/ndf
ISGW2	144 ± 44	$(1.00 \pm 0.31) \cdot 10^{-4}$	1.05
UKQCD	145 ± 44	$(1.20 \pm 0.37) \cdot 10^{-4}$	1.08
LCSR	176 ± 52	$(1.67 \pm 0.50) \cdot 10^{-4}$	1.04
average	$155 \pm 47 \pm 15$	$(1.29 \pm 0.39 \pm 0.28) \cdot 10^{-4}$	

TABLE II: The yield in the signal window, $763 < m(\pi^+ \pi^- \pi^0) < 803 \text{ MeV}/c^2$ and $|\Delta E| < 360 \text{ MeV}$, the corresponding branching fraction and the goodness of fit (estimated by the χ^2 divided by the number of degrees of freedom). For each fit (using a given form-factor model), the error quoted on the signal yield and the branching fraction is statistical only. For the average, the first error is statistical and the second is the spread around the central value.

RESULT AND SYSTEMATIC UNCERTAINTY

The fit is repeated for each of the three form-factor models available for $B^+ \rightarrow \omega l^+ \nu$. For each model, the signal yield, $N(B^+ \rightarrow \omega l^+ \nu)$, is determined and the branching ratio, $\mathcal{B}(B^+ \rightarrow \omega l^+ \nu)$, is calculated accordingly using the relation (Table II)

$$N(B^+ \rightarrow \omega l^+ \nu) = N(B^+) \times \mathcal{B}(B^+ \rightarrow \omega l^+ \nu) \times \mathcal{B}(\omega \rightarrow \pi^+ \pi^- \pi^0) \times (\epsilon_e + \epsilon_\mu). \quad (4)$$

$N(B^+)$ is the total number of charged B mesons in the data, $\mathcal{B}(\omega \rightarrow \pi^+ \pi^- \pi^0) = (89.1 \pm 0.7)\%$ [9] and ϵ_e (ϵ_μ) is the model-dependent selection efficiency for $\omega e \nu$ ($\omega \mu \nu$) candidates. Averaging over the three models (giving equal weight to each), a branching fraction of $(1.29 \pm 0.39) \cdot 10^{-4}$ is obtained. The spread around this average value, which amounts to $0.28 \cdot 10^{-4}$, is used as an estimate of the form-factor model uncertainty.

The quadratic sum of the experimental systematics (listed in Table III) is $0.21 \cdot 10^{-4}$ or 16.4% of the branching fraction. The largest contribution is the uncertainty in the $X_u l \nu$ cross-feed. It is estimated by separately varying the fraction of $B \rightarrow \pi l \nu$ and

	value	$\Delta\mathcal{B}/\mathcal{B}$	Ref.
$B^0 \rightarrow \pi^- l^+ \nu$	$(1.8 \pm 0.6) \cdot 10^{-4}$	2.2%	[9]
$B^0 \rightarrow \rho^- l^+ \nu$	$(2.6^{+0.6}_{-0.7}) \cdot 10^{-4}$	12.7%	[9]
other $B \rightarrow X_u l \nu$		1.4%	
$X_u l \nu$ cross-feed (sum)		13.0%	
neutrino reconstruction		4%	
charged track finding (l, π^+, π^-)		3%	
cluster finding (π^0)		4%	
(sum)		9%	
$X_c l \nu$ cross-feed		2.8%	
lepton identification		3.0%	
number of $B\bar{B}$	$(85.0 \pm 0.5) \cdot 10^6$	0.6%	
$\mathcal{B}(\omega \rightarrow \pi^+ \pi^- \pi^0)$	$(89.1 \pm 0.7)\%$	0.8%	[9]
total systematic uncertainty		16.4%	

TABLE III: Contributions to the systematic uncertainty. The size of each contribution is given as percentage of the branching ratio. The different components are discussed in the text.

$B \rightarrow \rho l \nu$ decays (that are expected to dominate in the high p_t^* region) within their respective experimental uncertainties. For the cross-feed from other $B \rightarrow X_u l \nu$ decays, the fit is repeated modeling this component once with the ISGW2 (fully resonant $B \rightarrow X_u l \nu$) and once with the De Fazio-Neubert model (fully non-resonant $B \rightarrow X_u l \nu$). Half of the difference between these two extreme cases is assigned as a systematic uncertainty.

The next largest component is the uncertainty in the neutrino reconstruction, track finding and cluster finding efficiency. Other contributions taken into account in the calculation of the systematic error are: $X_c l \nu$ cross-feed (estimated by varying the fraction of $B \rightarrow D^* l \nu$ in the $X_c l \nu$ component), lepton identification, the number of $B\bar{B}$ events and the uncertainty in the $\omega \rightarrow \pi^+ \pi^- \pi^0$ branching fraction.

CONCLUSION

We have studied the decay $B^+ \rightarrow \omega l^+ \nu$ using 78 fb^{-1} of $\Upsilon(4S)$ data (85.0 million $B\bar{B}$ events). The final state was reconstructed using the ω decay into $\pi^+ \pi^- \pi^0$ and detector hermeticity to infer the neutrino momentum. The signal yield and the remaining background were estimated by a binned maximum-likelihood fit. Repeating the fit for three different $B^+ \rightarrow \omega l^+ \nu$ form-factor models and averaging the result, 155 ± 47 signal events are found, corresponding to a branching fraction of $(1.3 \pm 0.4 \pm 0.2 \pm 0.3) \cdot 10^{-4}$, where the errors are statistical, systematic and estimated form-factor uncertainty, respectively. (This result is preliminary.)

ACKNOWLEDGEMENTS

We wish to thank the KEKB accelerator group for the excellent operation of the KEKB accelerator. We acknowledge support from the Ministry of Education, Culture, Sports, Science, and Technology of Japan and the Japan Society for the Promotion of Science; the Australian Research Council and the Australian Department of Education, Science and Training; the National Science Foundation of China under contract No. 10175071; the Department of Science and Technology of India; the BK21 program of the Ministry of Education of Korea and the CHEP SRC program of the Korea Science and Engineering Foundation; the Polish State Committee for Scientific Research under contract No. 2P03B 01324; the Ministry of Science and Technology of the Russian Federation; the Ministry of Education, Science and Sport of the Republic of Slovenia; the National Science Council and the Ministry of Education of Taiwan; and the U.S. Department of Energy.

* on leave from Fermi National Accelerator Laboratory, Batavia, Illinois 60510

† on leave from University of Pittsburgh, Pittsburgh PA 15260

‡ on leave from Nova Gorica Polytechnic, Nova Gorica

- [1] M. Kobayashi and T. Maskawa, *Prog. Theor. Phys.* **49**, 652 (1973).
- [2] Y. Kwon, *Proceedings 31st International Conference on High Energy Physics (ICHEP 2002)*, July 25-31, 2002, Amsterdam, The Netherlands, edited by S. Bentvelsen, P. de Jong, J. Koch and E. Laenen, ISBN 0-444-51343-4.
- [3] Throughout this article, the inclusion of the charge conjugate mode decay is implied.
- [4] A. Abashian *et al.* (Belle Collab.), *Nucl. Instr. and Meth.* **A 479**, 117 (2002).
- [5] N. Isgur and D. Scora, *Phys. Rev.* **D 52**, 2783 (1995). See also N. Isgur *et al.*, *Phys. Rev.* **D 39**, 799 (1989).
- [6] L. Del. Debbio *et al.*, *Phys. Lett.* **B 416**, 392 (1998).
- [7] P. Ball and V. M. Braun, *Phys. Rev.* **D 58**, 094016 (1998).
- [8] F. De Fazio, M. Neubert, *JHEP* **06**, 017 (1999).
- [9] K. Hagiwara *et al.*, *Phys. Rev.* **D66**, 010001 (2002).
- [10] G. C. Fox and S. Wolfram, *Phys. Rev. Lett.* **41**, 1581 (1978).
- [11] R. A. Fisher, *Annals of Eugenics* **7**, 179 (1936).
- [12] R. Barlow, C. Beeston, *J. Comp. Phys.* **72**, 202 (1987).